Technische Universität Darmstadt WS 2007/2008

Versuchsausarbeitung

Versuch 1.8
Infrarot-Spektroskopie

Bastian Löher und Antje Weber

November 2007

Betreuerin: Beata Walasek

Contents

1 Theoretical background

1.1 Fourier Transform Infrared Spectroscopy

A Fourier Transform Infrared spectrometer consists of a source of radiation, a beamsplitter and a detector. The core of a FT-IR spectrometer is a Michelson Interferometer which contains the beam splitter.

1.1.1 Light source

The light source in our FT-IR spectrometer is a ceramic compound. The emitted wavelength spectrum is dependent on the applied current.

1.1.2 Michelson Interferometer

The main components of a Michelson Interferometer are a beam splitter and two mirrors. The beam splitter splits the light into two beams perpendicular to each other. Each one of the beams travels through one arm of the interferometer and is reflected by the mirror. One of the two mirrors is moveable, therefore one way is variable. If the difference between the two ways is $\Delta s = \frac{k \cdot \lambda}{2}$ the beams show constructive interference. A Michelson Interferometer is used in the FT-IR spectrometer, because this way a precise interferogram can be produced. This interferogram can subsequently be fourier transformed into the transmission spectrum.

1.1.3 Detector

There are two different kinds of detectors. One is based on thermal detection of radiation. These detecors are very slow in detecting radiation but they are wavelength independent. The other type is a quantum detector. In these detectors the incoming radiation ejects electrons from the photomaterial, which are then detected. The advantage of quantum detectors is the fast detection of a signal, but at the same time the signal to noise ratio is worse compared to using thermal detectors.

1.1.4 Fourier Transformation and Apodisation

The Fourier Transformation is a transformation between the frequency domain and the space domain. The idea of the transformation is that all periodic functions can be written as an infinite sum of sines and cosines. This way we get a connection between the interferogram and the spectrum:

$$S(\nu) = \int_{-\infty}^{\infty} I(x) \cos(2\pi\nu x) dx \tag{1}$$

The interferogram is finite, because the way Δx of the variable mirror is limited. So the interferogram is incomplete, because both sides are cut off. We have to use a so called apodisation function. This function shapes the interferogram and helps to describe the outer

intervals which are not covered by our experimental data. We use the Boxcar function:

$$D(x) = \begin{cases} 1 & x \,\epsilon\, \{-x_{max}, x_{max}\} \\ 0 & \text{else} \end{cases} \tag{2}$$

the triangular function:

$$D(x) = 1 - \frac{|x|}{x_{max}} \quad x \,\epsilon\, \{-x_{max}, x_{max}\} \tag{3}$$

and the trapezoidal funcion:

$$D(x) = \begin{cases} 0 & x \leq x_a \,,\, x \geq x_d \\ 1 - \frac{|x|}{x_b} & x_a < x \leq x_b \\ 1 & x_b < x < x_c \\ 1 - \frac{|x|}{x_d} & x_c \leq x < x_d \end{cases} \quad \text{with } x_a < x_b < x_c < x_d \tag{4}$$

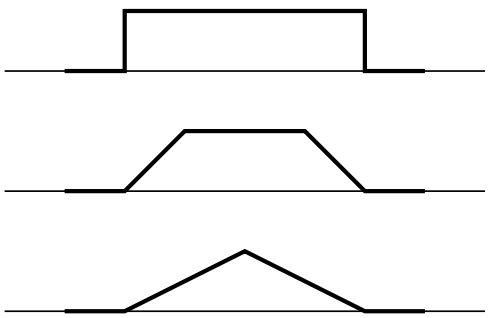

Figure 1: Different apodisation modes (boxcar, trapezoidal and triangular)

1.1.5 Eliminating background effects

To eliminate background effects we flood the sample chamber with N_2, because it is optically inactive. Each of the recorded spectra has to be divided by the background spectrum, because of the fact that the sample chamber still contains a great deal of optically active molecules.

1.2 Rotation and Vibration in Molecules

Generally the spectra of a molecule is composed of three components: the pure rotation spectrum, the rotation and vibration spectrum and the electronic spectrum. The whole stimulation energy is given by $E = E_{el} + E_{vib} + E_{rot}$. In the following sections we will have a look at the rotation and vibration energy.

1.2.1 Energy of rotation

The absorption can almost only be noticed in the rotation spectrum, because the probability of emission is very small at low frequencies. The selection rules allow only spectra with a permanent electric dipole moment to be observed. The energy of a rigid rotator which looks like a barbell is given by:

$$E_{rot} = \frac{1}{2}\Theta\omega^2 \tag{5}$$

with Θ = momentum of inertia. Insert the angular momentum $|L| = \Theta\omega$ into the energy of rotation

$$E_{rot} = \frac{|\vec{L}|^2}{2\Theta} \tag{6}$$

Because the angular momentum is quantized we write $|\vec{L}| = n\hbar \Rightarrow E_{rot} = \frac{n^2\hbar^2}{2\Theta}$, the eigenvalues of the angular momentum are $|\vec{L}| = \hbar\sqrt{n(n+1)}$. With $n = J$ we get

$$E_{rot} = \frac{\hbar^2}{2\Theta}J(J+1) \Rightarrow F(J) = \frac{E_{rot}}{hc} = \frac{h}{8\pi^2 c\Theta}J(J+1) \tag{7}$$

The value $\frac{h}{8\pi c\Theta}$ we call the rotation constant B. For later computations we write this equation in the following form:

$$\begin{gathered}
\nu = \nu_0 + B_1(J_1+1)J_1 - B_0J_0(J_0+1) \\
\nu_R : J_1 = J_0 + 1 = J + 1 \\
\nu_R(J) = \nu_0 + B_1(J+1)(J+2) - B_0J(J+1) \\
\nu_P : J_1 = J_0 - 1 = J - 1 \\
\nu_P(J) = \nu_0 + B_1(J-1)J - B_0J(J+1) \\
\nu_R(J) - \nu_P(J) = B_1(4J+2)
\end{gathered}$$

$$\Rightarrow B_1 = \frac{\nu_R(J) - \nu_P(J)}{2(2J+1)} \tag{8}$$

$$\begin{gathered}
\nu_P(J+2) = \nu_0 + B_1(J+1)(J+2) - B_0(J+2)(J+3) \\
\nu_R(J) - \nu_P(J+2) = B_0(4J+6)
\end{gathered}$$

$$\Rightarrow B_0 = \frac{\nu_R(J) - \nu_P(J+2)}{2(2J+3)} \tag{9}$$

$$B = \frac{3B_0 - B_1}{2} \tag{10}$$

$$\alpha = 2(B - B_0) \tag{11}$$

1.2.2 Vibrational Modes

The vibration spectrum is visible in the infrared spectral area, where the vivration frequencies of the molecule are. Here the probability of spontaneous emission is very small as well. Using the harmonic oscillator as a model we can calculate the energy of vibration:

$$E_{vib} = \hbar\omega\left(\nu + \frac{1}{2}\right) \Rightarrow G(\nu) = \frac{\omega}{2\pi c}\left(\nu + \frac{1}{2}\right) \tag{12}$$

The selection rules of the vibrations are $\Delta\nu = \pm 1$. The vibrations of homonucleic molecules are free of a dipolmoment, therefore there is no optical spectrum (e.g. nitrogen). That means that these molecules are optically inactive. If we look at the degrees of freedom, we get $3N$ possibilities for atoms to vibrate and 3 for rotation. The rotational degree of freedom is different for linear or non linear molecules. So we get:

$$f = 3N - 3 - \begin{cases} 2 & \text{linear} \\ 3 & \text{non linear} \end{cases} \tag{13}$$

The vibrations are divided in stretching and bending modes. Linear molecules have $N-1$ stretching and $2N-4$ bending modes, however non linear molecules have $N-1$ stretching and $2N-5$ bending modes. The stretching modes can be subdivided into symmetrical and antisymmetrical stretching modes.

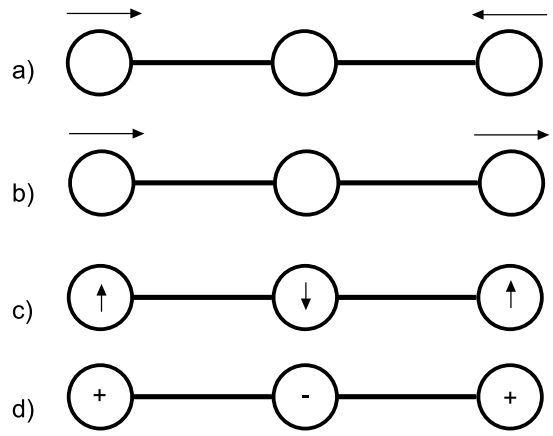

Figure 2: CO_2 vibrational modes. a) symmetric stretching mode. b) antisymmetric stretching mode. c) and d) bending modes perpendicular to each other and to the axis of symmetry.

2 Measurements

2.1 Differences between air and nitrogen

N_2 has some advantages over air when used as a medium in FT-IR spectroscopy. Being a 2-atom symmetrical molecule with a vanishing dipole moment, N_2 is not IR-active. Furthermore

it is a pure element and does not have any constituents with varying quantities. This makes it ideal for spectroscopy.

2.1.1 Interferometric differences

As we can see in fig. 3 the center burst of the interferogramm stays the same for air and nitrogen. The important differences can be found off to the sides of the spectrum (as seen in fig. 4), in the region further away from $\Delta s = 0$ in the interferometer. In the nitrogen interferogram we see much less fluctuations compared to the air interferogram.

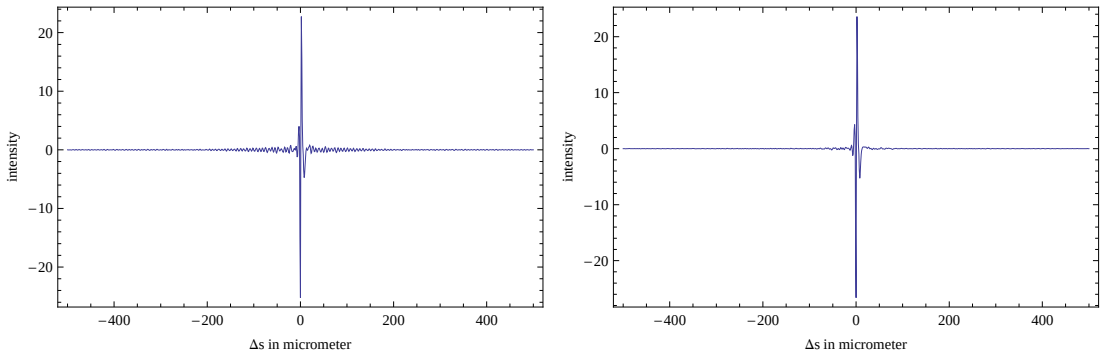

Figure 3: Interferograms of air (left) and nitrogen (right).

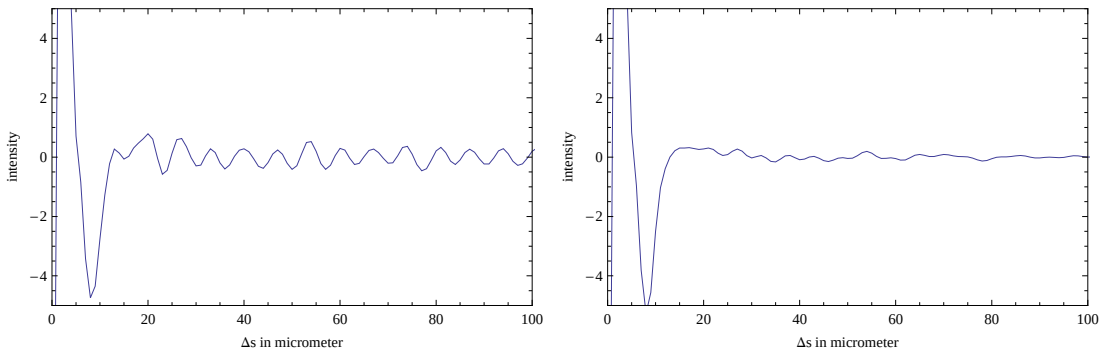

Figure 4: Enlarged area of the interferograms (Air on the left and nitrogen on the right).

2.1.2 Spectral differences

After appliying a fourier transform to the two interferograms we get the relative transmission as a function of frequency in units of cm^{-1}. In fig. 5 both spectra are plotted in the same diagram for better comparison. The nitrogen spectrum is displayed with an offset of +10%. It is clearly visible, that the nitrogen spectrum shows much less absorption, but at the same time we do see some peaks, even though nitrogen is not IR-active. Subsequently these peaks must result from the experimental setup, for example from absorption on the FT-IR surfaces and

the sample chamber, or from residual air in the setup. The spectrum itself mostly resembles the spectrum of a black-body radiator, even though we are only looking at a small portion of the usual black-body spectrum ranging from 0 to infinity.

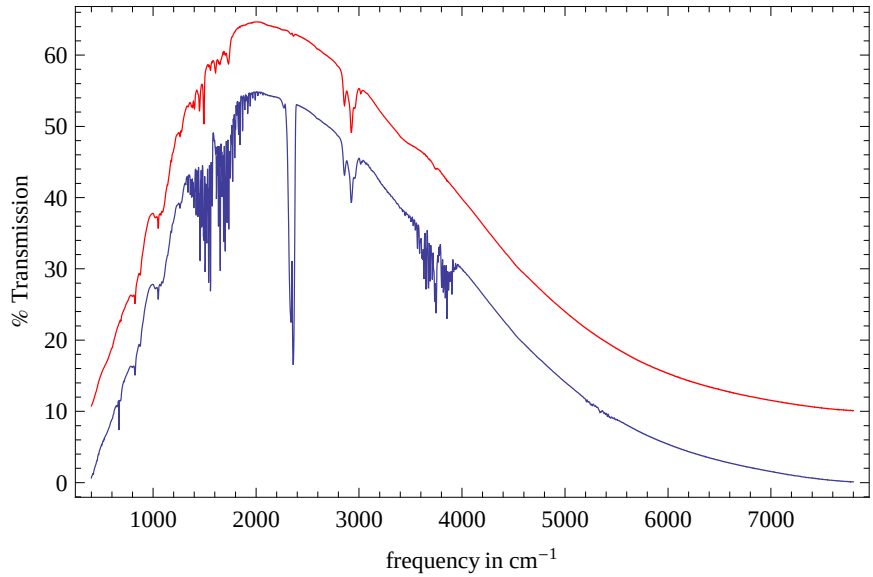

Figure 5: Spectra of air (blue) and nitrogen (red)

2.1.3 Constituents of air

If we devide the air spectrum by the nitrogen spectrum we receive a cleaned air spectrum (fig. 6), where only the constituents of air have visible peaks. The areas below 500 and above 6500 cm^{-1} yield no real information, because in these areas the spectra have been very similar and both close to zero. The most distinctive peaks can be observed around 670 cm^{-1}, 1600 cm^{-1}, 2350 cm^{-1} and 3750 cm^{-1}. A smaller one is visible at 5600 cm^{-1}.

Analysing the structure of those peaks we see nice P, Q and R branches in the first peak (fig. 7,l) at relatively low energy. This corresponds to the CO_2 perpendicular vibration mode with $\Delta J = 0$, because we see a Q line. The next peak is the first water absorption band for the bending mode. The water stretching modes look similar and are both located around 3750 cm^{-1} and are not magnified. The most interesting peak is the CO_2 antisymmetric stretching mode at 2350 cm^{-1}, but at the current resolution its fine structure can not be perceived.

2.2 Comparison of different apodisation functions

Using the CO_2 antisymmetric stretching mode's fine structure we compare the different settings for apodisation. In figure 8 the fine structure of the stretching mode is clearly visible. The blue line shows the mode with boxcar (rectangular) apodisation, whereas the green line has triangular apodisation applied. The lines we see here result from rotation states with even

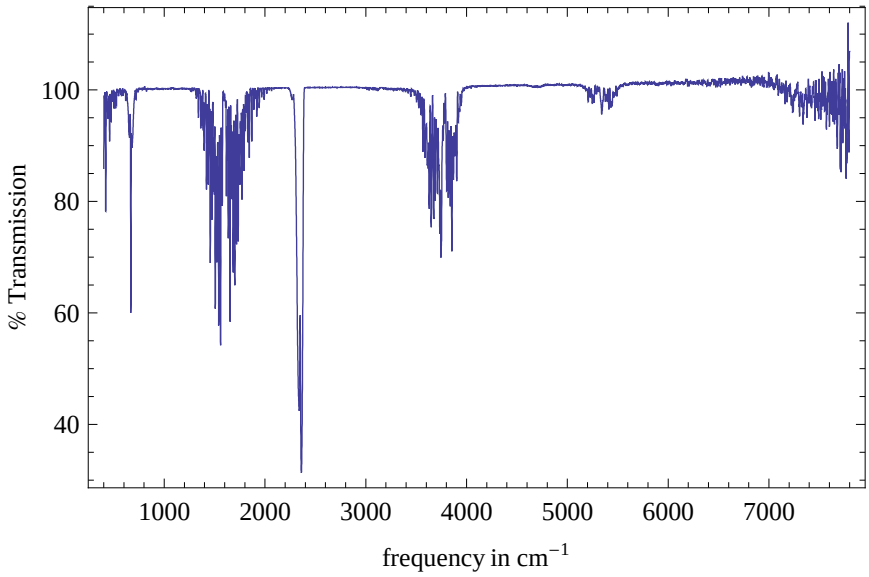

Figure 6: Cleaned spectrum of air

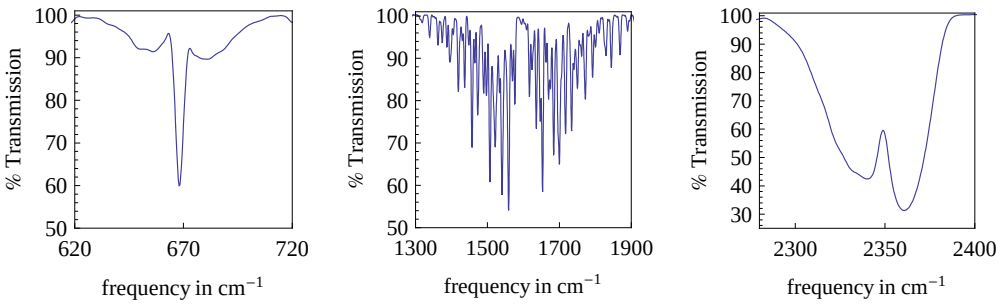

Figure 7: Constituents of air: (Left) Low energy CO_2 bending mode; (Middle) H_2O bending mode; (Right) CO_2 antisymmetric stretching mode.

quantum numbers only (e.g. $J = 0, 2, 4, ...$). This is due to the fact that CO_2 is a boson system with a total spin number $S = 0$. Boson systems have a symmetric wave function, so only symmetric rotation states can be populated as we see below:

$$\Psi_+ = Space \otimes Rotation \otimes Spin$$
$$\Psi_+ = \quad + \quad \otimes \quad + \quad \otimes \quad +$$

This leads to $\Delta J = \pm 2$ as the single selection rule for rotation states. The equations for calculating B_0 and B_1 have to be slightly adapted for calculating the rotation constant B and look like this:

$$\Rightarrow B_1 = \frac{\nu_R(J) - \nu_P(J)}{8J} \tag{14}$$

$$\Rightarrow B_0 = \frac{\nu_R(J) - \nu_P(J+2)}{4(2J+5)} \tag{15}$$

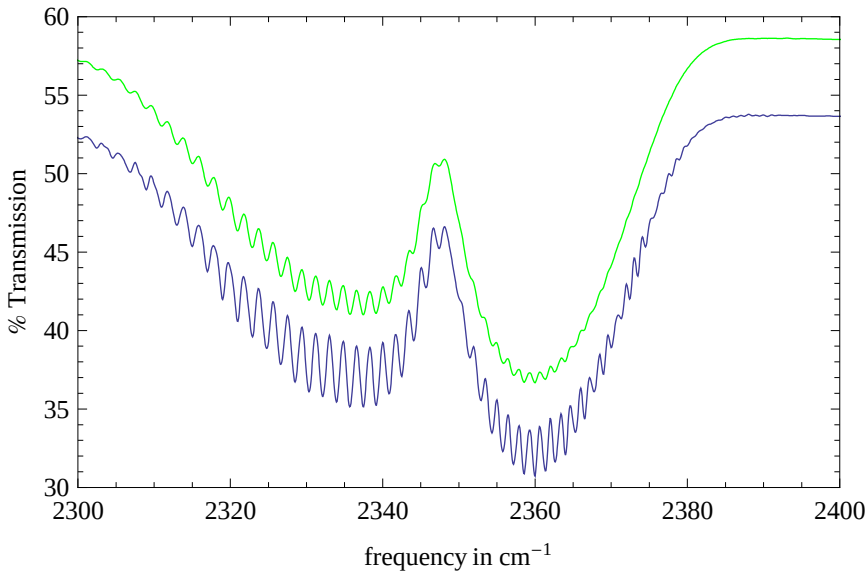

Figure 8: CO_2 lines at medium magnification with boxcar (blue) and triangular (green) apodisation.

In figure 9 an area of the above mode is enlarged showing now an additional setting of medium apodisation with a trapezoidal apodisation function. We can see that with stronger apodisation we lose some detail on the one hand, but on the other hand we gain clearer information about the important peaks and lose some of the ringing that originated from the fast fourier transform.

2.3 Analysis of different gases

In the next step we analysed 5 different gas spectrums of which we could only measure two by ourselves. The data for acetylene, carbon monoxide and methane came from other groups.

The interesting portion of the acetylene spectrum (fig. 10) shows splitting of each peak into two peaks of different intensity. This splitting occurs because of the fermi-nature of C_2H_2. This means that acetylene has a nuclear spin of either $S = 0$ or $S = 1$ resulting from the coupling of the hydrogen nulear spins of $s = \frac{1}{2}$ each. Also te wave function of acetylene must be antisymmetric. We can write the resulting wave function as follows

$$\Psi_- = Space \otimes Rotation \otimes Spin$$
$$\Psi_- = \quad + \quad \otimes \quad - \quad \otimes \quad +$$
$$\Psi_- = \quad + \quad \otimes \quad + \quad \otimes \quad -$$

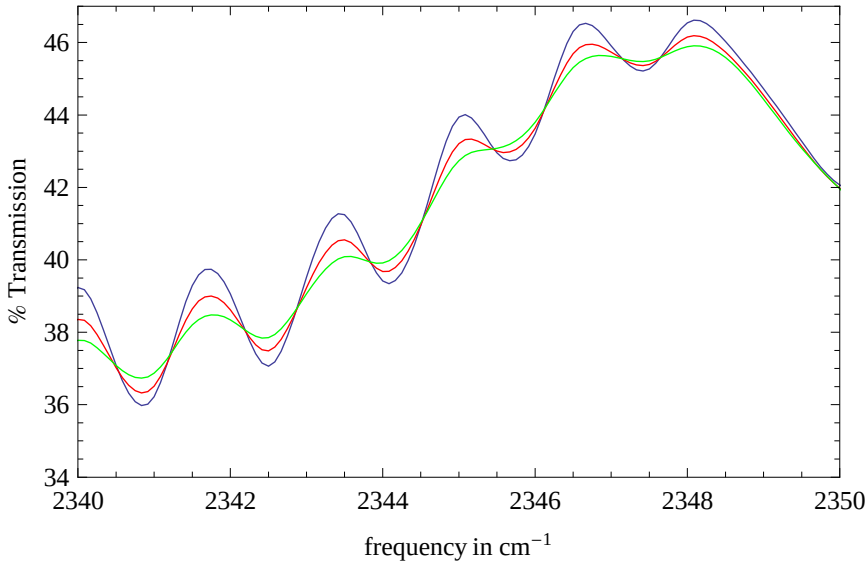

Figure 9: CO_2 lines at strong magnification with boxcar (blue), trapezoidal (red) and triangular (green) apodisation functions.

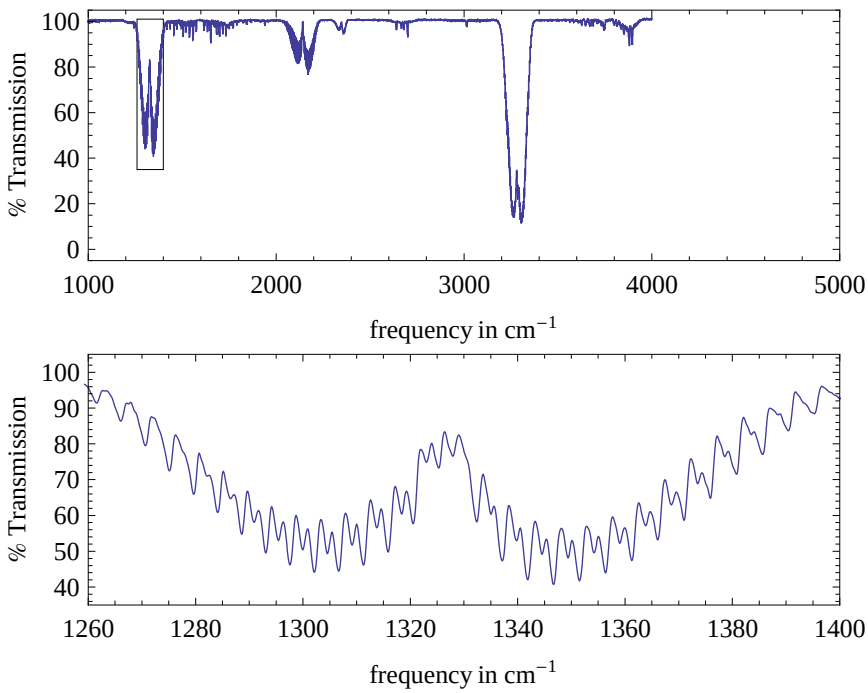

Figure 10: Spectrum of C_2H_2 and enlarged area with visible peak splitting

So we either have an antisymmetric rotation wave function with a symmetric spin wave function or vice versa. In the first case the angular momentum quantum number can obtain

the values $j = 1, 3, 5...$, while in the second case it can have the values $j = 0, 2, 4....$ The difference in intensity comes from the amount of multiplicity which is calculated by $n = 2S+1$, so the relation between the multiplicities is 1:3 resulting in three times higher population of the symmetric rotation states compared to the antisymmetric rotation. This again results in less intensity of those peaks.

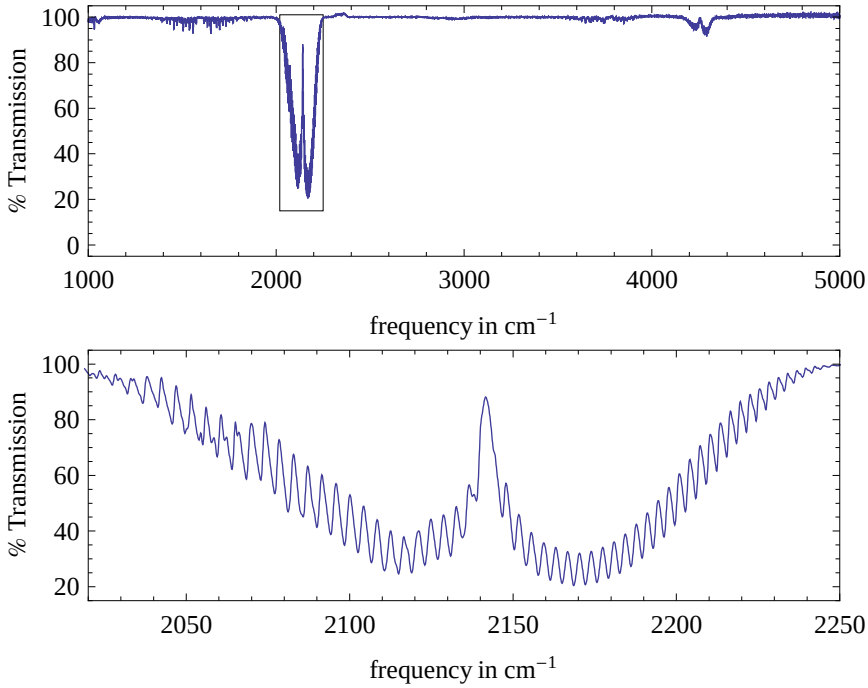

Figure 11: Spectrum of CO and enlarged area with non-splitting peaks

At a frequency of $2150cm^{-1}$ the CO spectrum (fig. 11) shows the symmetrical structure of a typical rotation vibration band. The other visible peak at $4260cm^{-1}$ is the first CO overtone.

In the CH_4 spectrum (fig. 12) the additional Q branch is also visible, resulting from the pure vibration transition.

The HCl spectrum (fig.13) shows another interesting phenomenon, because here we also have slightly splitted peaks. These do not result from nuclear spin influence, but instead from the presence of two different isotopes of of chlorine in the gas sample (^{35}Cl and ^{37}Cl). The slightly different masses change the angular momentum of the molecules and thus make a difference in the excitation energy.

2.4 Transmission of various glass samples

In figure 14 the transmission of seven different glass samples is shown.

blue Coated silicon shows contant transmission of around 10% and slightly better below $400cm^{-1}$.

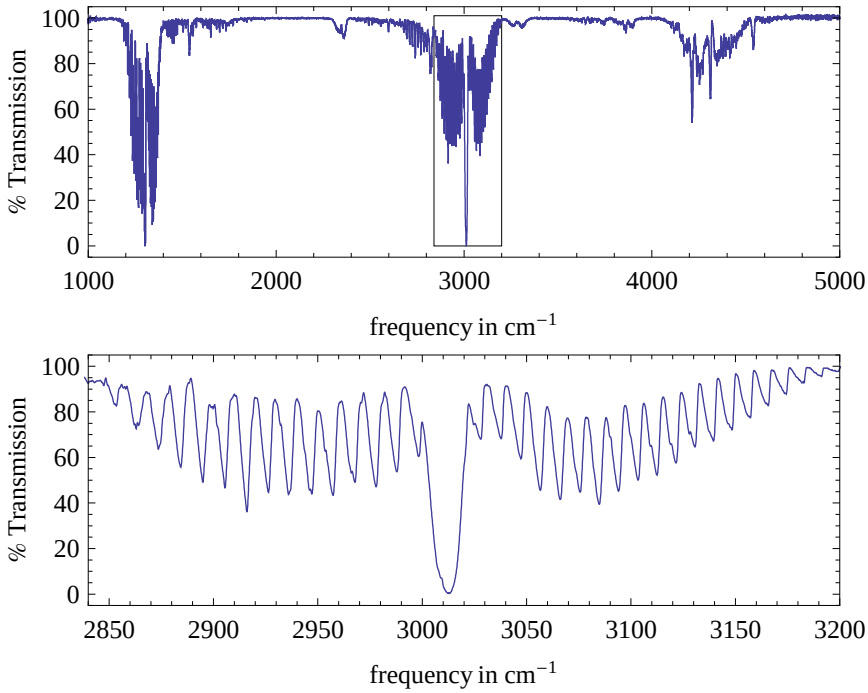

Figure 12: Spectrum of CH_4 and enlarged area with distinctive P, Q and R branches.

red Borosilicate shows no transmission up to $2000cm^{-1}$, but almost 100% at higher energies with an absorption line around $3650cm^{-1}$.

green Mica has some transmission below $1000cm^{-1}$ and 100% above this value. The oscillations we can see in the figure result from interference of the IR beam with itself on the thin mica sheet.

yellow Potassium bromide has almost constant transmission of 90%.

magenta Sapphire has no transmission below $1500cm^{-1}$ but then about 100% at higher energies similar to borosilicate.

cyan Silicon starts with 50% transmission and decreases in an almost linear fashion to about 25%.

gray Quartz glass has very similar transmission properties compared to borosilicate, but it does not have the peak around $3650cm^{-1}$.

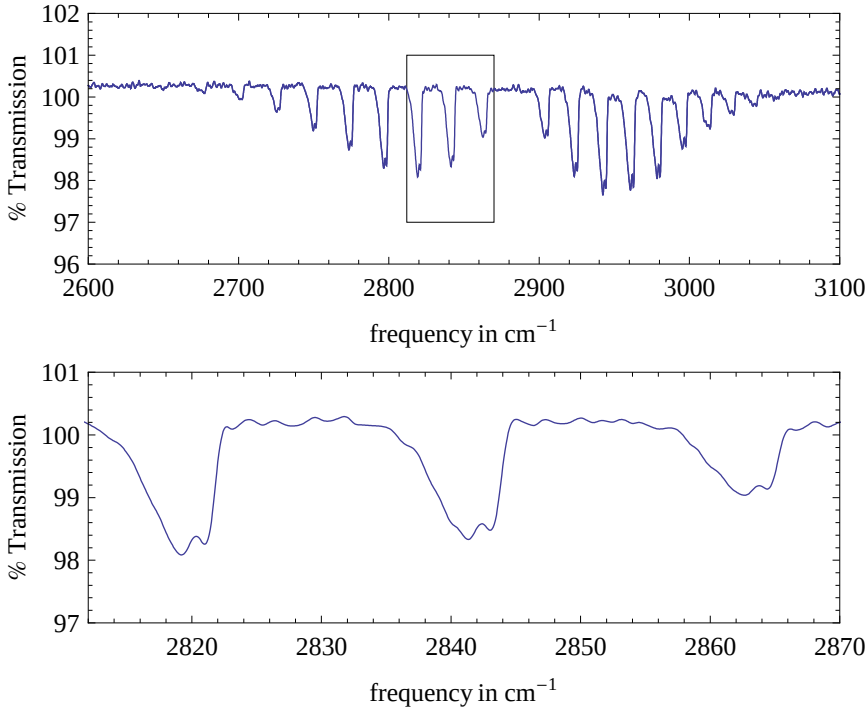

Figure 13: Hydrochloric acid (HCl) spectrum and enlarged area below.

3 Analysis

With the accumulated data we can calculate the rotational parameters B, B_0, B_1 and α as well as the momentum of inertia Θ, the reduced mass μ and the distance r between the atoms.

3.1 Rotational parameters

We can calculate the rotational parameters B, B_0, B_1 and α from the data of the CO, HCl, CH_4 and CO_2 molecules by looking at the frequency difference $\Delta\nu$ of corresponding peaks in the transmission spectra. Using the equations

$$B_1 = \frac{\nu_R(J) - \nu_P(J)}{2(2J+1)} \tag{16}$$

$$B_0 = \frac{\nu_R(J) - \nu_P(J+2)}{2(2J+3)} \tag{17}$$

$$B = \frac{1}{2}(3B_0 - B_1) \tag{18}$$

$$\alpha = 2(B - B_0) \tag{19}$$

we gain the following values for CO:

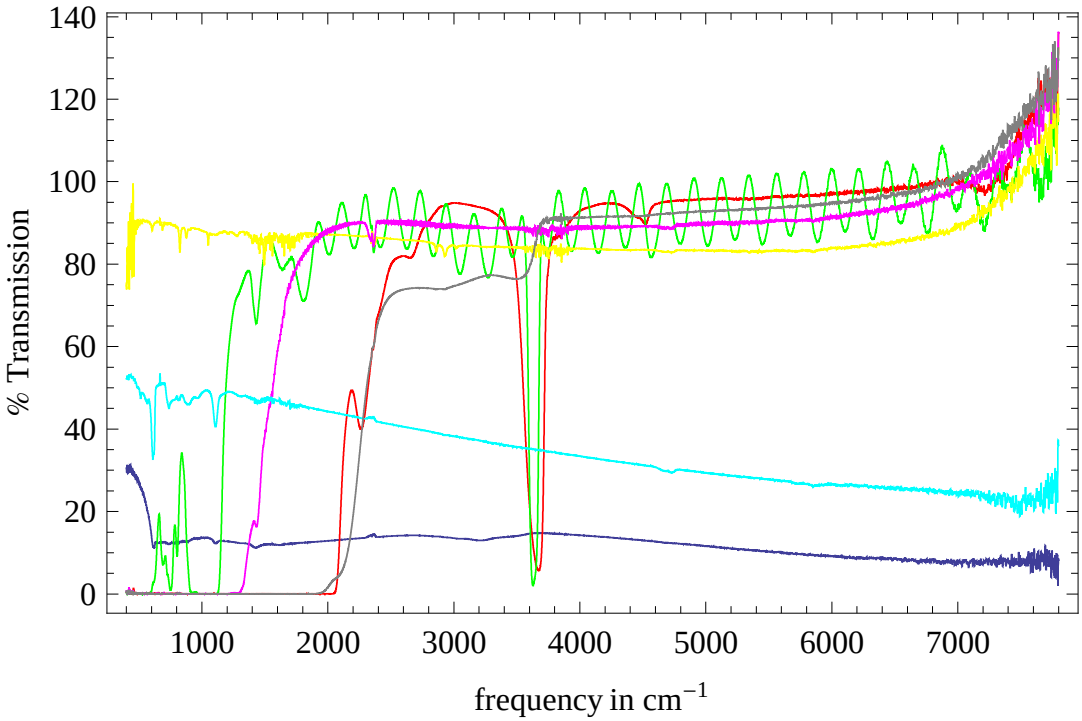

Figure 14: Transmission in various glass samples: (blue) coated silicon, (red) borosilicate, (green) mica, (yellow) potassium bromide, (magenta) sapphire, (cyan) silicon, (gray) quartz glass (SiO_2)

J	$\nu_P(J)$ $[cm^{-1}]$	$\nu_R(J)$ $[cm^{-1}]$	$\nu_P(J+2)$ $[cm^{-1}]$	B_1	B_0	B	α
0		2146.68	2134.54		2.023		
1	2138.24	2150.47	2130.78	2.038	1.969		
2	2134.54	2154.02	2126.88	1.948	1.939		
3	2130.78	2157.78	2122.92	1.929	1.937		
4	2126.88	2161.35	2118.96	1.915	1.927		
5	2122.92	2164.92		1.909			
Mean				1.948 $\pm$ 0.003	1.959 $\pm$ 0.002	1.965	0.011

and for HCl:

J	$\nu_P(J)$ $[cm^{-1}]$	$\nu_R(J)$ $[cm^{-1}]$	$\nu_P(J+2)$ $[cm^{-1}]$	B_1	B_0	B	α
1	2862.63	2923.71	2819.55	10.18	10.15	10.53	0.23
2	2841.32	2942.65	2796.82	10.13	10.42	10.56	0.29
3	2819.55	2961.12	2774.09	10.11	10.39	10.53	0.28
4	2796.82	2978.63	2750.41	10.10	10.37	10.51	0.28
5	2774.09	2996.16	2750.70	10.09	10.40	10.56	0.32
Mean				$10.12 \pm 1.27 \cdot 10^{-3}$	$10.35 \pm 1.23 \cdot 10^{-2}$	$10.54 \pm 4.75 \cdot 10^{-4}$	$0.28 \pm 1.05 \cdot 10^{-3}$

For CH_4 the values are:

J	$\nu_P(J)$ $[cm^{-1}]$	$\nu_R(J)$ $[cm^{-1}]$	$\nu_P(J+2)$ $[cm^{-1}]$	B_1	B_0	B	α
0		3027.55	2987.62		6.655		
1	2998.27	3037.82	2977.73	6.592	6.009		
2	2987.62	3046.94	2967.47	5.932	5.676		
3	2977.73	3056.07	2956.82	6.329	5.514		
4	2967.47	3065.95	2946.55	5.471	5.427		
5	2956.82	3075.46		5.393			
Mean				5.943 ± 0.274	5.856 ± 0.249	5.813	-0.086

and for CO_2:

J	$\nu_P(J)$ $[cm^{-1}]$	$\nu_R(J)$ $[cm^{-1}]$	$\nu_P(J+2)$ $[cm^{-1}]$	B_1	B_0	B	α
2	2343.85	2350.23	2342.39	0.399	0.218	0.128	-0.18
4	2342.39	2351.46	2340.78	0.283	0.205	0.166	-0.09
6	2340.78	2352.79	2339.02	0.250	0.203	0.180	-0.05
8	2339.02	2354.27	2337.55	0.238	0.199	0.180	-0.04
10	2337.55	2355.65	2335.71	0.226	0.199	0.186	-0.03
Mean				0.279 ± 0.070	0.204 ± 0.008	0.168 ± 0.024	0.078 ± 0.061

With the parameter B we can determine the momenta of inertia of the molecules using this equation which results from the definition of B

$$\Theta = \frac{h}{8\pi^2 cB} \tag{20}$$

Combining this value with the reduced mass μ we can further calculate the distance between the atoms in the molecules HCl and CO.

$$r = \sqrt{\frac{\Theta}{\mu}} \tag{21}$$

Molecule	Θ $[gcm^2]$	μ $[g]$	r [Å]
CO	1.425e-39	1.139e-23[1]	1.119
HCl	2.656e-40	1.627e-24[1]	1.278[2]

3.2 Molecular structure of Methanol

In figure 15 the spectrum of methanol shows several distinct absorption bands. From the position and shape of these bands we can determine the molecular structure of methanol. For this procedure we utilize several 'building bricks' with special absorption patterns. These bricks together with their absorption frequencies are displayed on the task sheet in chapter three.

$1030cm^{-1}$: This line probably corresponds to a $C-O$ group which has characteristic vibration frequencies in the range $1000-1200cm^{-1}$.

[1] The values for the reduced mass have been calculated using the atomic masses from P. A. Tipler: Physik, 1994

[2] This value differs only slightly from the literature such as Haken-Wolf, 4th edition: $r = 1.2746^{-10}m$

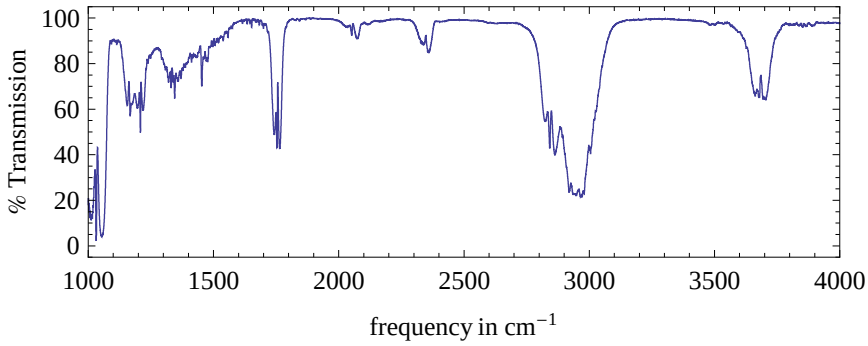

Figure 15: Methanol spectrum.

$1200cm^{-1}$ and $1450cm^{-1}$: These bands look like they are part of the characteristic spectrum of a CH_2 group which has absorption frequencies of $1300cm^{-1}$ and $1470cm^{-1}$

$1760cm^{-1}$ and $2050cm^{-1}$: There is no corresponding pattern on our task sheet that might correspond to the strong and the following weaker absorption band.

$2340cm^{-1}$: This is the CO_2 line from the surrounding air.

$2800cm^{-1}$ to $3100cm^{-1}$: These lines clearly belong to the $C-H$ pattern and the CH_3 pattern.

$3680cm^{-1}$: This line with some water background corresponds to the last puzzle piece which is the $O-H$ group.

Putting all the pieces together we can deduce that the molecular structure of methanol is CH_3OH.